JOURNAL OF MATERIALS PROCESSING TECHNOLOGY 197 (2008) 449–450

ELSEVIER

available at www.sciencedirect.com

ScienceDirect

journal homepage: www.elsevier.com/locate/jmatprotec

Author Index of Volume 197

Achyutha, B.T., 225
Aghakouchak, A.A., 140
Aid, A., 250
Alba, F., 161
Amrouche, A., 250
Ashkezari, G.D., 140
Attanasio, A., 59

Bamberg, E., 419
Banerjee, S., 306
Barrera, M.A., 221
Barreto, C., 161
Basheer, A.C., 439
Bera, J., 279
Bhanuprasad, V.V., 439
Bittencout, F.R., 344

Camurri, C.P., 292
Cao, M., 151
Casalino, G., 301
Ceretti, E., 59
Chang, C.-P., 284
Chen, C., 206
Chen, W., 36
Cheng, L., 170
Chou, C.P., 116
Cui, J., 109

Dabade, U.A., 439
Datta, C.K., 241
Dehlaghi, V., 174
Dong, Y., 31
Ducher, F., 10
Dutta, T., 306

Erdmann, M., 363

Feng, S., 296
Framinan, J.M., 1

Gadre, V.M., 439
Gaitonde, V.N., 225
Gandhi, A.H., 268
Gao, T., 255
Ger, M.-D., 284
Ghosal, S., 306
Giardini, C., 59
Gorni, A.A., 374
Grujicic, M., 363
Gu, X.-Y., 170
Guan, Y., 379
Guo, J., 101
Guo, Y.B., 189

Halali, M., 156
He, J., 31
Hiziroglu, S., 445
Holzleitner, J., 363
Hu, W., 77
Hu, X., 43, 206
Hua, Z.Z., 77
Huang, B.-C., 68
Huang, Y., 43
Huneau, B., 337
Hwu, W.-H., 284

Iida, Y., 261

Jha, G.C., 434
Jin, Q., 212
Jing, W., 54
Joshi, S.S., 439

Kan, S.M., 445
Kaneko, Y., 261
Kanno, Y., 261
Karnik, S.R., 225
Khamba, J.S., 200
Kim, H.S., 393
Koç, M., 393
Kokabi, M., 140
Kolhe, K.P., 241
Koric, S., 408
Kumruoglu, L.C., 182

Lai, H.W., 445
Li, J., 101
Li, W., 36
Li, X., 31
Li, Y., 325
Li, Y.-M., 170
Li, Z., 325
Liao, R.-H., 170
Lin, C.J., 445
Lin, F.-L., 68
Lin, H.-W., 284
Liu, H., 151
Liu, N., 36
Liu, X.Y., 428
Lu, H., 101, 206
Luan, B., 428
Ludovico, A.D., 301
Luo, D., 151

Maggiolino, S., 237
Mangalaraja, R.V., 292
Martínez-de-Pisón, F.J., 161
Martínez-Salazar, J., 221
Marya, S., 337
Mazzoni, L., 59
Mei, P.R., 374
Mesmacque, G., 250
Mukherjee, S.K., 17
Muñoz, A.C., 337
Muthukumaran, S., 17

Nagano, M.S., 1
Nagaumi, H., 109
Najarian, S., 174
Nath, A.K., 434
Ni, J., 393

Obieglo, A., 363
Omar, M.A., 363
Otto, M., 49
Özer, A., 182

Paramaputi, P., 132
Pernía, A., 161
Pourboghrat, F., 379

Qin, G.H., 122
Qu, J., 212

Rahmat, A.R., 22
Rakwal, D., 419
Ramam, K.V.S., 292
Raval, H.K., 268
Ravi, J., 292
Rojananan, S., 132
Roy, P.K., 279
Roy, S.K., 434
Rückert, G., 337

Sangghaleh, A., 156
Sasaki, T., 89
Sauvage, X., 337
Schmid, C., 237
Sedighi, M., 314
Sellappan, V., 363
Seyr, N., 363

Elsevier B.V.
doi:10.1016/S0924-0136(07)01355-6

Shadpoor, M.T., 174
Shen, Z., 151
Siddeswarappa, B., 225
Sin, L.T., 22
Singh, R., 200
Sinha, P., 17
Su, M., 250
Sun, H., 206

Tabourot, L., 10
Tan, G., 122
Thipprakmas, S., 132
Thomas, B.G., 408
Tokmechi, S., 314
Toussaint, F., 10

Vega, J.F., 221

Waikar, R.A., 189
Wan Abdul Rahman, W.A., 22
Wan, M., 122
Wan, Y., 96
Wang, C.-A., 43
Wang, H., 43
Wang, J.F., 428
Wang, J.-P., 68
Wang, S.C., 116
Wu, Z., 151

Xiong, D.-S., 96
Xu, B., 212
Xu, H., 296
Xu, W., 296
Xu, Z., 101

Yakou, T., 89
Yan, D., 31
Yang, H., 36, 206, 255, 296
Yao, L.G., 77
Yao, Z., 151
Yichao, D., 54
Yisan, W., 54
Yuli, L., 255
Yun, C.-C., 68

Zárate, L.E., 344
Zhang, J., 31
Zhang, R., 43
Zhang, W.H., 122
Zhang, Y.-P., 170
Zhang, Z., 325
Zhou, J., 325
Zhu, R., 325
Zuo, Y., 109

JOURNAL OF MATERIALS PROCESSING TECHNOLOGY 197 (2008) 451–457

available at www.sciencedirect.com

ScienceDirect

journal homepage: www.elsevier.com/locate/jmatprotec

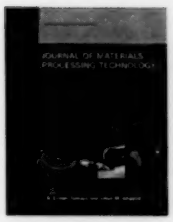

Subject Index of Volume 197

Activated TIG
Comparison of TIG welded and friction stir welded Al–4.5Mg–0.26Sc alloy, 337
Adaptive response surface method
Optimization of sheet metal forming processes by adaptive response surface based on intelligent sampling method, 77
Additional radial compressive stress
Extending the process limits at a collar forming process, 49
Air boundary layer
Development of a simple technique for improving the efficacy of fluid flow through the grinding zone, 306
Al–Mg–Sc alloy
Comparison of TIG welded and friction stir welded Al–4.5Mg–0.26Sc alloy, 337
Al_2O_3–TiO_2 coating
Microstructure characteristics of Al_2O_3–13 wt.% TiO_2 coating plasma spray deposited with nanocrystalline powders, 31
Alumina
An investigation on the wetting of polycrystalline alumina by aluminium, 156
Comparison of slurry effect on machining characteristics of titanium in ultrasonic drilling, 200
Aluminium
An investigation on the wetting of polycrystalline alumina by aluminium, 156
Aluminium alloy
Corrosion resistance in FSW and in MIG welding techniques of AA6XXX, 237
Aluminizing
Tool wear and surface roughness during machining of high-temperature aluminized steel, 89
Aluminum
Fourier series based finite element analysis of tube hydroforming—Generalized plane strain model, 379
Al–Zn–Mg–Cu alloy
Study on the sump and temperature field during low frequency electromagnetic casting a superhigh strength Al–Zn–Mg–Cu alloy, 109
Analytical model
Development of an analytical model for warm deep drawing of aluminum alloys, 393
Analytical study
Analytical and empirical modeling of top roller position for three-roller cylindrical bending of plates and its experimental verification, 268
Anisotropic behaviour
Experimental and numerical analysis of the forming process of a CP titanium scoliotic instrumentation, 10
Artificial neural networks
Modeling of surface roughness in precision machining of metal matrix composites using ANN, 439
Asymmetric parts
Asymmetric two points incremental forming: Improving surface quality and geometric accuracy by tool path optimization, 59
Automotive structural components
An overview of the polymer-to-metal direct-adhesion hybrid technologies for load-bearing automotive components, 363

Backward simulation
Influence of dynamic boundary conditions on preform design for deformation uniformity in backward simulation, 255
Bauxite tailings
Influence of heat-treatment schedule on crystallization and microstructure of bauxite tailing glass–ceramics coated on tiles, 206
Bending
Experimental and numerical analysis of the forming process of a CP titanium scoliotic instrumentation, 10
Betel palm stem
Manufacturing particleboard panels from betel palm (*Areca catechu* Linn.), 445
Boron carbide
Comparison of slurry effect on machining characteristics of titanium in ultrasonic drilling, 200
Buckling mechanism
Study of edge effect and multi-curvature in laser bending of AISI 304 stainless steel, 434
Burr size
Genetic algorithm-based burr size minimization in drilling of AISI 316L stainless steel, 225

CAD–CAM design
Asymmetric two points incremental forming: Improving surface quality and geometric accuracy by tool path optimization, 59
Ce^{3+}
Magnetic properties of Ce,Gd-substituted yttrium iron garnet ferrite powders fabricated using a sol–gel method, 296
Central composite rotatable design of experiments
Genetic algorithm-based burr size minimization in drilling of AISI 316L stainless steel, 225

Elsevier B.V.
doi:10.1016/S0924-0136(07)01356-8

Ceramics
Processing and dielectric properties of Bi-doped $Sr(Ti_{0.95}Zr_{0.05})O_3$ ceramics, 151
Characterization of nanocrystalline NiCuZn ferrite powders synthesized by sol–gel auto-combustion method, 279
Coating
Influence of heat-treatment schedule on crystallization and microstructure of bauxite tailing glass–ceramics coated on tiles, 206
Cold rolling process
Representation and control of the cold rolling process through artificial neural networks via sensitivity factors, 344
Collar forming process
Extending the process limits at a collar forming process, 49
Composite
Characterization of a powder metallurgy SiC/Cu–Al composite, 43
Computational fluid dynamics
Analysis of wall shear stress in stented coronary artery using 3D computational fluid dynamics modeling, 174
Computer simulation
Investigation of critical liquid fraction factor in nodular iron castings by computer simulation, 182
Constitutive model
Parameter identification of superplastic constitutive model by GA-based global optimization method, 212
A mixtures-based model for the grain size dependent mechanical behavior of nanocrystalline materials, 325
Constitutive models
Thermo-mechanical models of steel solidification based on two elastic visco-plastic constitutive laws, 408
Contact analysis
Fourier series based finite element analysis of tube hydroforming—Generalized plane strain model, 379
Contact angle
An investigation on the wetting of polycrystalline alumina by aluminium, 156
Controlled rolling
Effect of controlled-rolling parameters on the ageing response of HSLA-80 steel, 374
Coolant supply nozzle
Development of a simple technique for improving the efficacy of fluid flow through the grinding zone, 306
Copper
Effect of controlled-rolling parameters on the ageing response of HSLA-80 steel, 374
Coronary artery
Analysis of wall shear stress in stented coronary artery using 3D computational fluid dynamics modeling, 174
Co-rotating twin-screw extruder
Three-dimensional modelling of flow curves in co-rotating twin-screw extruder elements, 221
Corrosion
Corrosion resistance in FSW and in MIG welding techniques of AA6XXX, 237
Cutting force model
Systematic simulation procedure of peripheral milling process of thin-walled workpiece, 122
Cutting temperature
Tool wear and surface roughness during machining of high-temperature aluminized steel, 89
CVN test
Prediction of microstructure and mechanical properties of multipass SAW, 241

3D numerical simulation
Three-dimensional modelling of flow curves in co-rotating twin-screw extruder elements, 221
Data mining
Modelling of an elastomer profile extrusion process using support vector machines (SVM), 161
DC casting
Study on the sump and temperature field during low frequency electromagnetic casting a superhigh strength Al–Zn–Mg–Cu alloy, 109
Deep drawing
Development of an analytical model for warm deep drawing of aluminum alloys, 393
Deformation uniformity
Influence of dynamic boundary conditions on preform design for deformation uniformity in backward simulation, 255
Degree of cold expansion
Numerical study of the optimum degree of cold expansion: Application for the pre-cracked specimen with the expanded hole at the crack tip, 250
Density
Characterization of a powder metallurgy SiC/Cu–Al composite, 43
Dielectric properties
Processing and dielectric properties of Bi-doped $Sr(Ti_{0.95}Zr_{0.05})O_3$ ceramics, 151
Discharge energy density
Experimental investigation of wire electrical discharge machining of gallium-doped germanium, 419
Drilling
Genetic algorithm-based burr size minimization in drilling of AISI 316L stainless steel, 225

ECAE
Effect of adding Sc and Zr on grain refinement and ductility of AZ31 magnesium alloy, 116
Edge effect
Study of edge effect and multi-curvature in laser bending of AISI 304 stainless steel, 434
Elastic behavior
A mixtures-based model for the grain size dependent mechanical behavior of nanocrystalline materials, 325
Elastic-visco-plastic material
Thermo-mechanical models of steel solidification based on two elastic visco-plastic constitutive laws, 408
Elastomer extrusion
Modelling of an elastomer profile extrusion process using support vector machines (SVM), 161
Electrical discharge machining
Experimental investigation of wire electrical discharge machining of gallium-doped germanium, 419
Electrical properties
Characterization of nanocrystalline NiCuZn ferrite powders synthesized by sol–gel auto-combustion method, 279
Electrochromic devices
Fabrication of pulsed-laser deposited V_2O_5 thin films for electrochromic devices, 261
Electromechanical properties
Piezoelectric and dielectric properties of $PbNb_2O_6$-based piezoelectric ceramics with high Curie temperature, 170

Electrostatic separation
Movement behavior in electrostatic separation: Recycling of metal materials from waste printed circuit board, 101
Empirical modeling
Analytical and empirical modeling of top roller position for three-roller cylindrical bending of plates and its experimental verification, 268
Equivalent von Mises stress
Numerical study of the optimum degree of cold expansion: Application for the pre-cracked specimen with the expanded hole at the crack tip, 250
Extended process limits
Extending the process limits at a collar forming process, 49

FEM
Influence of dynamic boundary conditions on preform design for deformation uniformity in backward simulation, 255
Ferrite
Magnetic properties of Ce,Gd-substituted yttrium iron garnet ferrite powders fabricated using a sol–gel method, 296
Fe–(Ti,V)C composite
Reaction synthesis of Fe–(Ti,V)C composites, 54
Fiber reinforced elastomeric isolator
Design, manufacturing and evaluation of the performance of steel like fiber reinforced elastomeric seismic isolators, 140
Finite element analysis
Finite element simulation of high speed pulse welding of high specific strength metal alloys, 301
Development of an analytical model for warm deep drawing of aluminum alloys, 393
Finite element method (FEM)
An investigation of step taper-shaped punch in piercing process using finite element method, 132
Finite element model
Performance of Ti(C,N)-based cermets cutter and simulation technique of cutting process, 36
Finite elements
Three-dimensional modelling of flow curves in co-rotating twin-screw extruder elements, 221
Fourier series based finite element analysis of tube hydroforming—Generalized plane strain model, 379
Thermo-mechanical models of steel solidification based on two elastic visco-plastic constitutive laws, 408
Finite volume method
A new approach to preform design in forging process of complex parts, 314
Flow analysis
Injection moulding simulation analysis of natural fiber composite window frame, 22
Flowshop
Evaluating the performance for makespan minimisation in no-wait flowshop sequencing, 1
Forging
A new approach to preform design in forging process of complex parts, 314
Fourier series
Fourier series based finite element analysis of tube hydroforming—Generalized plane strain model, 379
Friction stir welding
Analysis of first mode of metal transfer in friction stir welded plates by image processing technique, 17
Friction stir welding
Corrosion resistance in FSW and in MIG welding techniques of AA6XXX, 237
Comparison of TIG welded and friction stir welded Al–4.5Mg–0.26Sc alloy, 337
Frictional performance
The effect of laser surface texturing on frictional performance of face seal, 96
Fusion welding
Comparison of TIG welded and friction stir welded Al–4.5Mg–0.26Sc alloy, 337
F-value approach
A new experimental approach to evaluate friction in ring test, 68

Gd^{3+}
Magnetic properties of Ce,Gd-substituted yttrium iron garnet ferrite powders fabricated using a sol–gel method, 296
Genetic algorithm
Genetic algorithm-based burr size minimization in drilling of AISI 316L stainless steel, 225
Glass–ceramic
Influence of heat-treatment schedule on crystallization and microstructure of bauxite tailing glass–ceramics coated on tiles, 206
Global optimization
Parameter identification of superplastic constitutive model by GA-based global optimization method, 212
Grain refinement
Effect of adding Sc and Zr on grain refinement and ductility of AZ31 magnesium alloy, 116
Grinding zone fluid flow
Development of a simple technique for improving the efficacy of fluid flow through the grinding zone, 306

Heat-affected zone
Prediction of microstructure and mechanical properties of multipass SAW, 241
Heat-treatment schedule
Influence of heat-treatment schedule on crystallization and microstructure of bauxite tailing glass–ceramics coated on tiles, 206
Heuristic algorithm
Evaluating the performance for makespan minimisation in no-wait flowshop sequencing, 1
High Curie temperature
Piezoelectric and dielectric properties of $PbNb_2O_6$-based piezoelectric ceramics with high Curie temperature, 170
High specific strength alloys
Finite element simulation of high speed pulse welding of high specific strength metal alloys, 301
High speed pulse welding
Finite element simulation of high speed pulse welding of high specific strength metal alloys, 301
High speed steel
Comparison of slurry effect on machining characteristics of titanium in ultrasonic drilling, 200
Horizontal test
Design, manufacturing and evaluation of the performance of steel like fiber reinforced elastomeric seismic isolators, 140
HSLA-80 steel
Effect of controlled-rolling parameters on the ageing response of HSLA-80 steel, 374

Image processing
Analysis of first mode of metal transfer in friction stir welded plates by image processing technique, 17
A new experimental approach to evaluate friction in ring test, 68
Improved preform
A new approach to preform design in forging process of complex parts, 314
In situ generation
Reaction synthesis of Fe–(Ti,V)C composites, 54
Increased hole expansion ratio
Extending the process limits at a collar forming process, 49
Injection moulding
Injection moulding simulation analysis of natural fiber composite window frame, 22
Instantaneous uncut chip thickness
Systematic simulation procedure of peripheral milling process of thin-walled workpiece, 122
Intermetallic compound
Tool wear and surface roughness during machining of high-temperature aluminized steel, 89
Inverse analysis
Parameter identification of superplastic constitutive model by GA-based global optimization method, 212

Laser bending
Study of edge effect and multi-curvature in laser bending of AISI 304 stainless steel, 434
Laser texturing
The effect of laser surface texturing on frictional performance of face seal, 96
Lead metaniobate
Piezoelectric and dielectric properties of $PbNb_2O_6$-based piezoelectric ceramics with high Curie temperature, 170
Lightweight material
Development of an analytical model for warm deep drawing of aluminum alloys, 393
Liquid fraction
Investigation of critical liquid fraction factor in nodular iron castings by computer simulation, 182
Low frequency electromagnetic field
Study on the sump and temperature field during low frequency electromagnetic casting a superhigh strength Al–Zn–Mg–Cu alloy, 109

Machinability
Tool wear and surface roughness during machining of high-temperature aluminized steel, 89
Machining
A comprehensive characterization of 3D surface topography induced by hard turning versus grinding, 189
Magnesium alloys
Effect of adding Sc and Zr on grain refinement and ductility of AZ31 magnesium alloy, 116
Magnetic materials
Characterization of nanocrystalline NiCuZn ferrite powders synthesized by sol–gel auto-combustion method, 279
Magnetic properties
Characterization of nanocrystalline NiCuZn ferrite powders synthesized by sol–gel auto-combustion method, 279
Magnetic properties of Ce,Gd-substituted yttrium iron garnet ferrite powders fabricated using a sol–gel method, 296
Makespan
Evaluating the performance for makespan minimisation in no-wait flowshop sequencing, 1
Material removal rate
Comparison of slurry effect on machining characteristics of titanium in ultrasonic drilling, 200
Measurement by strain gage
A new experimental approach to evaluate friction in ring test, 68
Mechanical properties
Comparison of TIG welded and friction stir welded Al–4.5Mg–0.26Sc alloy, 337
Metal cutting
Tool wear and surface roughness during machining of high-temperature aluminized steel, 89
Metal flow
Analysis of first mode of metal transfer in friction stir welded plates by image processing technique, 17
Metal materials
Movement behavior in electrostatic separation: Recycling of metal materials from waste printed circuit board, 101
Metal matrix composites design of experiments
Modeling of surface roughness in precision machining of metal matrix composites using ANN, 439
Metamodel
Optimization of sheet metal forming processes by adaptive response surface based on intelligent sampling method, 77
Microhardness
Prediction of microstructure and mechanical properties of multipass SAW, 241
Micropore
The effect of laser surface texturing on frictional performance of face seal, 96
Microstructure
Microstructure characteristics of Al_2O_3–13 wt.% TiO_2 coating plasma spray deposited with nanocrystalline powders, 31
Characterization of a powder metallurgy SiC/Cu–Al composite, 43
Reaction synthesis of Fe–(Ti,V)C composites, 54
Comparison of TIG welded and friction stir welded Al–4.5Mg–0.26Sc alloy, 337
Microwave-citrate-gel decomposition
Synthesis of nanocrystalline yttria by microwave-assisted citrate-gel decomposition technique, 292
Moldflow
Injection moulding simulation analysis of natural fiber composite window frame, 22
Multi-curvature
Study of edge effect and multi-curvature in laser bending of AISI 304 stainless steel, 434

Nanocrystalline
Synthesis of nanocrystalline yttria by microwave-assisted citrate-gel decomposition technique, 292
Nanocrystalline materials
A mixtures-based model for the grain size dependent mechanical behavior of nanocrystalline materials, 325
Nanoparticles
Magnetic properties of Ce,Gd-substituted yttrium iron garnet ferrite powders fabricated using a sol–gel method, 296
Nanostructured coatings
Microstructure characteristics of Al_2O_3–13 wt.% TiO_2 coating plasma spray deposited with nanocrystalline powders, 31

Natural fiber composite
Injection moulding simulation analysis of natural fiber composite window frame, 22
Neural networks
Representation and control of the cold rolling process through artificial neural networks via sensitivity factors, 344
Nodular cast iron
Investigation of critical liquid fraction factor in nodular iron castings by computer simulation, 182
No-wait
Evaluating the performance for makespan minimisation in no-wait flowshop sequencing, 1
Numerical simulation
Experimental and numerical analysis of the forming process of a CP titanium scoliotic instrumentation, 10
Performance of Ti(C,N)-based cermets cutter and simulation technique of cutting process, 36

Optimum rake angle
Performance of Ti(C,N)-based cermets cutter and simulation technique of cutting process, 36

Parameter identification
Parameter identification of superplastic constitutive model by GA-based global optimization method, 212
Parametric design
A new approach to preform design in forging process of complex parts, 314
Particle shape
Movement behavior in electrostatic separation: Recycling of metal materials from waste printed circuit board, 101
Particle swarm optimization intelligent sampling
Optimization of sheet metal forming processes by adaptive response surface based on intelligent sampling method, 77
Particleboard
Manufacturing particleboard panels from betel palm (*Areca catechu* Linn.), 445
Paste
The rheological behaviors of screen-printing pastes, 284
Peripheral milling
Systematic simulation procedure of peripheral milling process of thin-walled workpiece, 122
Phase analysis
Prediction of microstructure and mechanical properties of multipass SAW, 241
Piercing
An investigation of step taper-shaped punch in piercing process using finite element method, 132
Piezoelectric properties
Piezoelectric and dielectric properties of $PbNb_2O_6$-based piezoelectric ceramics with high Curie temperature, 170
Plane strain
Fourier series based finite element analysis of tube hydroforming—Generalized plane strain model, 379
Plasma spray
Microstructure characteristics of Al_2O_3–13 wt.% TiO_2 coating plasma spray deposited with nanocrystalline powders, 31
Plastic deformation
A mixtures-based model for the grain size dependent mechanical behavior of nanocrystalline materials, 325
Polymer impregnation
Fabrication of Ti/polymer biocomposites for load-bearing implant applications, 428
Polymer metal adhesion
An overview of the polymer-to-metal direct-adhesion hybrid technologies for load-bearing automotive components, 363
Polymer metal hybrids
An overview of the polymer-to-metal direct-adhesion hybrid technologies for load-bearing automotive components, 363
Porous Ti
Fabrication of Ti/polymer biocomposites for load-bearing implant applications, 428
Position of instability
Numerical study of the optimum degree of cold expansion: Application for the pre-cracked specimen with the expanded hole at the crack tip, 250
Powder metallurgy
Characterization of a powder metallurgy SiC/Cu–Al composite, 43
Reaction synthesis of Fe–(Ti,V)C composites, 54
Precipitation hardening
Effect of controlled-rolling parameters on the ageing response of HSLA-80 steel, 374
Predictive model
Representation and control of the cold rolling process through artificial neural networks via sensitivity factors, 344
Preform design
Influence of dynamic boundary conditions on preform design for deformation uniformity in backward simulation, 255
Principal components analysis
Modelling of an elastomer profile extrusion process using support vector machines (SVM), 161
Printed circuit board
Movement behavior in electrostatic separation: Recycling of metal materials from waste printed circuit board, 101
Pulsed-laser deposition
Fabrication of pulsed-laser deposited V_2O_5 thin films for electrochromic devices, 261
PV value
The effect of laser surface texturing on frictional performance of face seal, 96

Real-time measuring
A new experimental approach to evaluate friction in ring test, 68
Recycling
Movement behavior in electrostatic separation: Recycling of metal materials from waste printed circuit board, 101
Regeneration mechanism
Systematic simulation procedure of peripheral milling process of thin-walled workpiece, 122
Response surface methodology
Genetic algorithm-based burr size minimization in drilling of AISI 316L stainless steel, 225
Restenosis
Analysis of wall shear stress in stented coronary artery using 3D computational fluid dynamics modeling, 174
Rheology
The rheological behaviors of screen-printing pastes, 284

Rice husk
Injection moulding simulation analysis of natural fiber composite window frame, 22
Ring test
A new experimental approach to evaluate friction in ring test, 68
Roller bending
Analytical and empirical modeling of top roller position for three-roller cylindrical bending of plates and its experimental verification, 268
Rolling
Effect of adding Sc and Zr on grain refinement and ductility of AZ31 magnesium alloy, 116

SAW
Prediction of microstructure and mechanical properties of multipass SAW, 241
Scandium
Effect of adding Sc and Zr on grain refinement and ductility of AZ31 magnesium alloy, 116
Screen-printing
The rheological behaviors of screen-printing pastes, 284
Seismic isolation
Design, manufacturing and evaluation of the performance of steel like fiber reinforced elastomeric seismic isolators, 140
Sessile drop
An investigation on the wetting of polycrystalline alumina by aluminium, 156
Shaving
An investigation of step taper-shaped punch in piercing process using finite element method, 132
Shear stress
Analysis of wall shear stress in stented coronary artery using 3D computational fluid dynamics modeling, 174
Sheet metal forming
Optimization of sheet metal forming processes by adaptive response surface based on intelligent sampling method, 77
SiC/Cu–Al
Characterization of a powder metallurgy SiC/Cu–Al composite, 43
Silicon carbide
Comparison of slurry effect on machining characteristics of titanium in ultrasonic drilling, 200
Single crystal germanium
Experimental investigation of wire electrical discharge machining of gallium-doped germanium, 419
Sintering
Fabrication of Ti/polymer biocomposites for load-bearing implant applications, 428
Slicing rate
Experimental investigation of wire electrical discharge machining of gallium-doped germanium, 419
Solidification
Investigation of critical liquid fraction factor in nodular iron castings by computer simulation, 182
Solidification and melting
Thermo-mechanical models of steel solidification based on two elastic visco-plastic constitutive laws, 408
Springback
Analytical and empirical modeling of top roller position for three-roller cylindrical bending of plates and its experimental verification, 268
Stainless steel
Comparison of slurry effect on machining characteristics of titanium in ultrasonic drilling, 200
Static form error
Systematic simulation procedure of peripheral milling process of thin-walled workpiece, 122
Steel casting
Thermo-mechanical models of steel solidification based on two elastic visco-plastic constitutive laws, 408
Steel industry
Representation and control of the cold rolling process through artificial neural networks via sensitivity factors, 344
Stent
Analysis of wall shear stress in stented coronary artery using 3D computational fluid dynamics modeling, 174
Strontium titanate
Processing and dielectric properties of Bi-doped $Sr(Ti_{0.95}Zr_{0.05})O_3$ ceramics, 151
Subsurface damage
Experimental investigation of wire electrical discharge machining of gallium-doped germanium, 419
Sump
Study on the sump and temperature field during low frequency electromagnetic casting a superhigh strength Al–Zn–Mg–Cu alloy, 109
Support vector machines
Modelling of an elastomer profile extrusion process using support vector machines (SVM), 161
Surface integrity
A comprehensive characterization of 3D surface topography induced by hard turning versus grinding, 189
Surface roughness
Modeling of surface roughness in precision machining of metal matrix composites using ANN, 439
Surface topography
A comprehensive characterization of 3D surface topography induced by hard turning versus grinding, 189
Synthesis
Synthesis of nanocrystalline yttria by microwave-assisted citrate-gel decomposition technique, 292

Taper punch
An investigation of step taper-shaped punch in piercing process using finite element method, 132
Temperature field
Study on the sump and temperature field during low frequency electromagnetic casting a superhigh strength Al–Zn–Mg–Cu alloy, 109
Temperature gradient mechanism
Study of edge effect and multi-curvature in laser bending of AISI 304 stainless steel, 434
Temperature measurement
Study on the sump and temperature field during low frequency electromagnetic casting a superhigh strength Al–Zn–Mg–Cu alloy, 109
Thermo-mechanical processes
Thermo-mechanical models of steel solidification based on two elastic visco-plastic constitutive laws, 408
Thin film
Fabrication of pulsed-laser deposited V_2O_5 thin films for electrochromic devices, 261

Thin-walled workpiece
Systematic simulation procedure of peripheral milling process of thin-walled workpiece, 122
Ti/polymer composites
Fabrication of Ti/polymer biocomposites for load-bearing implant applications, 428
Ti(C,N)-based cermets
Performance of Ti(C,N)-based cermets cutter and simulation technique of cutting process, 36
Titanium
Experimental and numerical analysis of the forming process of a CP titanium scoliotic instrumentation, 10
Comparison of slurry effect on machining characteristics of titanium in ultrasonic drilling, 200
Tool life
Tool wear and surface roughness during machining of high-temperature aluminized steel, 89
Tool path optimization
Asymmetric two points incremental forming: Improving surface quality and geometric accuracy by tool path optimization, 59
Tool wear
Tool wear and surface roughness during machining of high-temperature aluminized steel, 89
Tool wear rate
Comparison of slurry effect on machining characteristics of titanium in ultrasonic drilling, 200
Tube hydroforming
Fourier series based finite element analysis of tube hydroforming—Generalized plane strain model, 379
Turning
Tool wear and surface roughness during machining of high-temperature aluminized steel, 89
Two points incremental forming
Asymmetric two points incremental forming: Improving surface quality and geometric accuracy by tool path optimization, 59

Ultimate stress
Numerical study of the optimum degree of cold expansion: Application for the pre-cracked specimen with the expanded hole at the crack tip, 250
Ultrasonic drilling
Comparison of slurry effect on machining characteristics of titanium in ultrasonic drilling, 200
Uncertainty analysis
Analytical and empirical modeling of top roller position for three-roller cylindrical bending of plates and its experimental verification, 268
Urea formaldehyde resin
Manufacturing particleboard panels from betel palm (*Areca catechu* Linn.), 445

Vertical test
Design, manufacturing and evaluation of the performance of steel like fiber reinforced elastomeric seismic isolators, 140
Virtual sensor
Representation and control of the cold rolling process through artificial neural networks via sensitivity factors, 344
V_2O_5
Fabrication of pulsed-laser deposited V_2O_5 thin films for electrochromic devices, 261

Warm forming
Development of an analytical model for warm deep drawing of aluminum alloys, 393
Wetting
An investigation on the wetting of polycrystalline alumina by aluminium, 156
Window frame
Injection moulding simulation analysis of natural fiber composite window frame, 22

YIG
Magnetic properties of Ce,Gd-substituted yttrium iron garnet ferrite powders fabricated using a sol–gel method, 296
Yttria
Synthesis of nanocrystalline yttria by microwave-assisted citrate-gel decomposition technique, 292

Zirconium
Effect of adding Sc and Zr on grain refinement and ductility of AZ31 magnesium alloy, 116